in selection and use of the sample support, P. J. Ihrig, G. G. Jones, Eric Jagel, and Carl Myerholtz, Standard Oil Co., for varied contributions to the development of optimal mass spectral and related computing procedures, H. M. Levy, State University of New York, for an enzymatic hydrolysis, as noted in footnote 60, and R. D. Grigsby, Texas A&M University, and R. D. Minard, The Pennsylvania State University, for allowing us access to unpublished material.

Registry No. Adenosine 5′-triphosphate, 56-65-5; [γ-^{18}O]adenosine 5′-triphosphate, 73116-39-9.

Supplementary Material Available: Tables giving data on treatment of P_i with water to test for oxygen exchange (Table I), isotopic analyses over the indicated time spans of two products from reactions of PCl_5 with $H_2{}^{18}O$ (Table II), isotopic analyses via GC/MS and probe/MS (Table III), isotopic analysis of P_i from reaction of PCl_5 with $H_2{}^{18}O$ (Table IV), isotopic analysis of P_i from reaction of PCl_5 with $H_2{}^{18}O$ (Table V), and calculation of ATP P_γ isotopic composition from analysis of P_i from hydrolysis in which the resultant P_i retains three of the four P_γ oxygen atoms and acquires one from water (Table VI), and figure showing evolution of methanol, water, and trimethyl phosphate from probe packed with 5-Å molecular sieve (Figure 1) (8 pages). Ordering information is given on ay current masthead page.

Conformational Studies of *S*-Adenosyl-L-homocysteine, a Potential Inhibitor of *S*-Adenosyl-L-methionine-Dependent Methyltransferases[1]

Toshimasa Ishida,*† Atsuko Tanaka,† Masatoshi Inoue,† Takaji Fujiwara,‡ and Ken-ichi Tomita‡

Contribution from the Osaka College of Pharmacy, Matsubara-City, Osaka 580, Japan, and the Faculty of Pharmaceutical Sciences, Osaka University, Yamadaoka, Suita, Osaka 565, Japan.
Received March 22, 1982

Abstract: The spatially favored conformation of *S*-adenosyl-L-homocysteine (SAH), a potent inhibitor of *S*-adenosyl-L-methionine (SAM) dependent methyltransferases, was studied by X-ray diffraction, 200-MHz ^{1}H nuclear magnetic resonance (NMR), and theoretical methods. The crystal used for X-ray analysis was monoclinic, of space group $C2$, with a = 45.942 (16) Å, b = 5.687 (1) Å, c = 15.627 (6) Å, β = 100.28 (5)°, and Z = 8. The final R index was 0.12 for 3243 independent reflections measured by Cu Kα radiation. The conformation of two crystallographically independent molecules was anti for the glycosyl bond, C(3′)-endo– or C(1′)-exo–C(2′)-endo sugar puckering, gauche/gauche for the orientation about the C(4′)–C(5′) bond, trans or gauche$^+$ about the C(α)–C(β) bond, trans about the C(β)–C(γ) bond, and gauche$^-$ or gauche$^+$ about the C(γ)–S bond. On the other hand, analysis of ^{1}H NMR spectra in ^2H_2O and $(C^2H_3)_2SO$ solutions showed a lack of conformational preference and approximately equal populations of rotational isomers. For elucidation of the energetically stable conformation of the SAH molecule, classical potential energy calculations were carried out, using the minimization technique. Each of the rotatable bonds varied for C(3′)-endo or C(2′)-endo ribose puckering. The torsion angles about the glycosyl, C(4′)–C(5′) and C(5′)–S bonds are highly important for energetically favored conformations. The SAH molecule favors two types of conformers for C(2′)-endo and three types for C(3′)-endo ribose puckering; the latter conformers are energetically less favorable by about 2–3 kcal/mol.

Biological transmethylation reactions are usually achieved by methyltransferases, utilizing *S*-adenosyl-L-methionine (SAM) as a methyl donor. *S*-Adenosyl-L-homocysteine (SAH), a demethylated metabolite of SAM, can bind to these methyltransferases and potentially inhibit their catalytic reaction. These enzymes are restimulated by adenosylhomocysteinase, which degrades SAH.[2] In tissue, the SAH and SAM level is equivalent;[3,4] therefore, SAH may be a key molecule in the regulatory mechanism of biological transmethylation.[5-7]

For elucidation of the functional groups of SAH necessary for inhibition and for development of more potent inhibitors, inhibitory experiments of SAH analogues have been performed for many methyltransferases such as catechol *O*-methyltransferase, hydroxyindole *O*-methyltransferase, and transfer RNA methyltransferase.[8-10] These enzymes generally show strict specificity for the structural features of SAH; the functional groups of primary importance for binding to the enzymes are terminal carboxyl (a) and amino (b) groups, sulfur atom (c), hydroxyl groups (d), and the amino group of the adenine base (e).[11]

Knowledge about the spatial arrangement of these functional groups is necessary to elucidate the substrate specificity of methyltransferases.

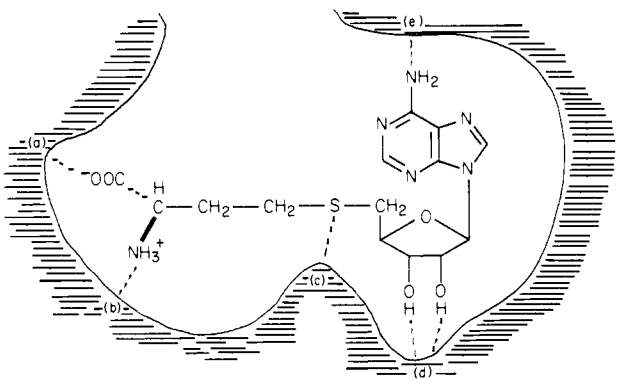

We now report the crystal structure of the SAH molecule as determined by the X-ray diffraction method and discuss the

† Osaka College of Pharmacy.
‡ Osaka University.

(1) Preliminary results for X-ray analysis were reported in *J. Chem. Soc., Chem. Commun.* 671 (1981).
(2) For reviews, see: F. Salvatore et al., "The Biochemistry of *S*-Adenosylmethionine", Columbia University Press, New York, 1977; S. K. Shapiro, F. Schlenk, Eds., "Transmethylation and Methionine Biosynthesis", University of Chicago Press, Chicago, 1965.
(3) F. Salvatore, R. Utili, V. Zappia, and S. K. Shapiro, *Anal. Biochem.*, **41**, 16 (1971).

0002-7863/82/1504-7239$01.25/0

Table I. Crystal Data

	crystal form I	crystal form II
molecular formula	$C_{14}H_{20}O_5N_6S\cdot 2.75H_2O$[a]	$C_{14}H_{20}O_5N_6S\cdot 2.75H_2O$
space group	$C2$	$C2$
a, Å	44.942 (16)	45.942 (16)
b, Å	5.638 (1)	5.687 (1)
c, Å	31.206 (9)	15.627 (6)
β, deg	95.95 (5)	100.28 (5)
Z	16	8
V, Å^3	7865 (3)	4017 (2)
d_{obsd}, g cm^{-3}	1.452 (1)	1.440 (1)
d_{calcd}	1.466	1.435

[a] Number of waters of crystallization was determined from thermal analysis.

preferred conformations, which were investigated by ^{1}H NMR analyses and classical potential energy calculations.

Experimental Section

Structural Change of SAH Crystals. Transparent, thin needle crystals of SAH, purchased from Boehringer Mannheim (W. Germany), were obtained from aqueous solution by slow evaporation at room temperature. Analytical data and thermal analysis of the fresh crystals indicated the presence of 2.75 waters of crystallization per molecule. As all efforts to obtain well-grown crystals failed, we used a 0.04 × 0.5 × 0.2 mm crystal for X-ray studies. Preliminary oscillation and Weissenberg and precession photographs indicated the crystal to be monoclinic. Systematic absences, (hkl) reflections for $h + k$ odd, ($h0l$) for h odd, and ($0k0$) for k odd, disclosed the space group to be $C2$, Cm, or $C2/m$. As the SAH molecule has asymmetric carbons, its space group is $C2$.

During X-ray data collection, using the crystal without mother liquor, the intensity of two out of four standard reflections, monitored at 100-reflection intervals, decreased rapidly. The Weissenberg photograph of this crystal showed the absence of hkl reflections for l odd and a minor change in the a and b cell constants. This structural change suggests that two kinds of SAH crystalline forms are derived from the aqueous solution (the former is subsequently referred to as I, the latter as II). In fact, crystals of form II were obtained when crystals of form I were stored for 1 month in the presence of the mother liquor. Although SAH undergoes spontaneous oxidation to *S*-adenosyl-L-homocysteine sulfoxide during preparation or storage,[12] infrared spectra[13] demonstrated that both crystal forms contain intact SAH molecules. On the other hand, when crystal form II was sealed in a glass capillary with some mother liquor and X-ray irradiated, it reversed to form I. These observations imply that the structural change is due to a difference of crystal packing, especially a difference in hydrogen bonding modes between SAH molecules and waters of crystallization.

Crystal data for both crystal forms are summarized in Table I. The cell parameters were determined by least-squares fitting of the setting angles for 12 reflections on a Rigaku automated four-circle diffractometer, using graphite-monochromated Cu Kα radiation. As crystal form II has the same space group as form I, the decrease by about one-half of the latter volume is indicative of the convergence of the number of independent molecules in the asymmetric unit from four to two, in the absence of a large conformational change of the respective SAH molecules.

Structure Determination and Refinement of Crystal Form II. A single 0.04 × 0.5 × 0.2 mm crystal of form I, obtained by X-ray irradiation, was used for data collection. A total of 4018 unique intensities ($\sin\theta/\lambda \leq 0.60$) were collected by the ω–2θ scan mode on the diffractometer with graphite-monochromated Cu Kα radiation. The scan speed was 2°/min with 5-s backgrounds measured at the two extremes of the scan. No net structural damage was observed in the intensities of four standard reflections measured after every 100 reflections. The data were subjected to Lorentz and polarization corrections; no correction was applied for absorption. For structure determination and refinement, 3243 reflections above the background level were used.

Repeated attempts to solve the structure by the direct method with the MULTAN78 program[14] were unsuccessful, probably due to the poor starting set for obtaining the phase relation of the remaining reflections. Therefore, we determined the phases of the additional 58 reflections by manual calculation, using the symbolic addition procedure[15] in terms of two starting signs and six symbols. These initial phases were used as the input for the tangent formula, and the phases for the remaining 516 reflections having large E values ($|E| \geq 1.42$) were computed. Based on a phase set having the highest combined figure of merit, the electron density map revealed an adenine ring and two sulfur atoms. The remaining atoms were obtained by several cycles of difference electron density calculations. All of the 58 non-hydrogen atoms were refined by the block-diagonal least-squares technique with anisotropic thermal parameters (program HBLS V[16]). A total of 40 hydrogen atom positions, excluding those of waters, were included in the structure calculations, but these were not refined. The final R index $[(\sum||R_o| - |F_c||)/(\sum|F_o|)]$ was 0.12.[17] The minimized function was $\sum w(|F_o| - |F_c|)^2$ with $w = [\sigma^2(F_o) + a|F_o| + b|F_o|^2]^{-1}$, where $\sigma(F_o)$ is the standard deviation based on counting statistics and a and b are −0.61651 and 0.02913 Å, respectively. The atomic scattering factors were taken from ref 18. All numerical calculations were performed on an ACOS-700 computer at the Crystallographic Research Center, Institute for Protein Research, Osaka University. Table II contains the final positional and thermal parameters of all the non-hydrogen atoms of two crystallographically independent SAH molecules (molecules A and B) and waters of crystallization.

Conformational Study by Proton Magnetic Resonance (^{1}H NMR). ^{1}H NMR spectra at 25 °C were obtained on a Varian XL-200(200-MHz, FT mode) spectrometer. Chemical shifts were measured vs. internal Me_4Si, tetramethylsilane, for $(C^2H_3)_2SO$ solution or DSS, 4,4-dimethyl-4-silapentanesulfonate, for ^2H_2O solution. Samples were adjusted to 0.087 M.

The SAH conformation was analyzed in accordance with the conventional methods, using the observed chemical shifts (δ) and the coupling constant (J).

In nucleosides and nucleotides, stable conformations about the glycosyl bond are found in both the anti and syn ranges. We utilized the chemical shifts of ribose protons for semiquantitative evaluation of the conformation about the glycosyl bond.[19-21] With a syn ⇌ anti dynamic equilibrium, rapid on the NMR time scale, the chemical shifts of the ribose protons are expressed by

$$\delta_{obsd} = P_{syn}\delta_{syn} + P_{anti}\delta_{anti}$$

where δ_{obsd} represents the observed chemical shifts, δ_{syn} and δ_{anti} the chemical shifts for the extreme syn and anti conformations, and P_{syn} and P_{anti} the populations of these conformations. The conformer populations about the glycosyl bond of SAH were analyzed based on the observed chemical shift (ppm) of H(2′), which is most sensitive to a conformational change for syn (δ 5.02 ppm, in $(C^2H_3)_2SO$ solution, 5.24 ppm in ^2H_2O solution) to anti (δ 4.22 ppm in $(C^2H_3)_2SO$ solution, 4.40 ppm in ^2H_2O solution).[19]

(4) J. Hoffman, *Anal. Biochem.*, **68**, 522 (1975).
(5) T. Deguchi and J. Barchas, *J. Biol. Chem.*, **246**, 3175 (1971).
(6) A. Oliva, P. Galletti, and V. Zappia, *Eur. J. Biochem.*, **104**, 595 (1980).
(7) P. M. Ueland and J. Saebø, *Biochemistry*, **18**, 4130 (1979).
(8) J. K. Coward, P. L. Bussolotti, and C. D. Chang, *J. Med. Chem.*, **17**, 1286 (1974).
(9) R. T. Borchardt, J. A. Huber, and Y. S. Wu, *J. Med. Chem.*, **17**, 868 (1974).
(10) R. T. Borchardt and Y. S. Wu, *J. Med. Chem.*, **17**, 862 (1974).
(11) R. T. Borchardt and Y. S. Wu, *J. Med. Chem.*, **18**, 300 (1975).
(12) J. A. Duerre, *Arch. Biochem. Biophys.*, **96**, 70 (1962).
(13) J. A. Duerre, L. Salisbury, and C. H. Miller, *Anal. Biochem.*, **35**, 505 (1970).
(14) P. Main, S. E. Hull, L. Lessinger, G. Germain, J. P. Declercq, and M. M. Woolfson, "MULTAN 78, a System of Computer Programs for the Automatic Solution of Crystal Structure from X-ray Diffraction Data", University of York, York, England, 1978.
(15) J. Karle and I. L. Karle, *Acta Crystallogr.*, **21**, 849 (1966).
(16) T. Ashida, "UNICS-Osaka", The Computation Center, Osaka University, Osaka, Japan, 1979.
(17) The final R value is relatively high, probably due to the small size of the used crystal, and the interconversion between forms I and II. In the last cycle of refinement, no parameters shifted more than one-fifth of the estimated deviations. The residual fluctuations in the difference Fourier map were within the range from −0.45 to 0.40 e Å^{-3}. After submission of this manuscript an independent determination of this crystal structure (form II) was reported by H. S. Shieh and H. M. Berman (*Acta Crystallogr., Sect. B*, **38**, 1513 (1982)).
(18) "International Tables for X-ray Crystallography", Vol. IV, Kynoch Press, Birmingham, England, 1974.
(19) R. Stolarski, A. Pohorille, L. Dudycz, and D. Shugar, *Biochim. Biophys. Acta*, **610**, 1 (1980).
(20) R. Stolarski, L. Dudycz, and D. Shugar, *Eur. J. Biochem.*, **108**, 111 (1980).
(21) L. Dudycz, R. Stolarski, R. Pless, and D. Shugar, *Z. Naturforsch., C: Biosci.* **34**, 359 (1979).

Table II. Positional (×10⁴) and Thermal (×10) Parameters of Non-Hydrogen Atoms

atom	*x*	*y*	*z*	B_{eq},[a] Å²
		Molecule A		
N(1)	3646 (3)	3203 (25)	4226 (8)	50 (3)
C(2)	3506 (3)	1907 (39)	4735 (9)	61 (4)
N(3)	3336 (2)	144 (30)	4511 (8)	51 (3)
C(4)	3303 (2)	−408 (30)	3672 (8)	38 (3)
C(5)	3433 (2)	650 (33)	3048 (8)	41 (3)
C(6)	3624 (2)	2632 (27)	3340 (8)	39 (3)
N(6)	3748 (2)	3970 (26)	2844 (7)	49 (3)
N(7)	3351 (2)	−309 (24)	2274 (6)	47 (3)
C(8)	3183 (3)	−2105 (28)	2400 (9)	54 (4)
N(9)	3148 (2)	−2205 (25)	3233 (7)	46 (3)
C(1′)	2957 (3)	−3919 (37)	3658 (9)	58 (4)
O(1′)	2877 (2)	−5740 (26)	3009 (7)	61 (3)
C(2′)	2685 (3)	−2782 (52)	3875 (11)	52 (3)
O(2′)	2597 (3)	−4048 (43)	4545 (9)	89 (5)
C(3′)	2457 (3)	−3529 (43)	3030 (10)	66 (5)
O(3′)	2169 (2)	−3552 (41)	3117 (9)	85 (4)
C(4′)	2569 (3)	−6070 (45)	2723 (11)	60 (4)
C(5′)	2504 (3)	−6616 (39)	1844 (14)	68 (5)
S	2535 (1)	−4383 (14)	1012 (3)	64 (1)
C(γ)	2161 (4)	−3165 (39)	794 (13)	65 (4)
C(β)	1961 (3)	−4500 (35)	81 (9)	49 (3)
C(α)	1641 (3)	−3795 (23)	49 (8)	37 (2)
N(α)	1468 (2)	−5415 (20)	−601 (7)	43 (2)
C(1)	1561 (3)	−1331 (27)	−213 (8)	39 (3)
O(1)	1418 (3)	−812 (23)	−947 (8)	69 (3)
O(2)	1639 (4)	248 (31)	320 (9)	92 (5)
		Molecule B		
N(1)	4273 (2)	535 (23)	5608 (5)	29 (2)
C(2)	4440 (3)	2380 (26)	5377 (7)	38 (3)
N(3)	4498 (2)	2806 (22)	4617 (5)	31 (2)
C(4)	4388 (2)	1202 (20)	4016 (6)	29 (2)
C(5)	4222 (2)	−806 (23)	4161 (6)	30 (2)
C(6)	4163 (2)	−1077 (22)	5016 (6)	29 (2)
N(6)	4012 (2)	−2821 (25)	5234 (6)	42 (2)
N(7)	4142 (2)	−2039 (23)	3394 (6)	35 (2)
C(8)	4257 (3)	−795 (26)	2835 (6)	31 (2)
N(9)	4404 (2)	1131 (17)	3166 (5)	31 (2)
C(1′)	4536 (2)	2884 (22)	2657 (6)	24 (2)
O(1′)	4321 (2)	3600 (17)	1936 (4)	33 (2)
C(2′)	4798 (2)	2002 (23)	2292 (6)	28 (2)
O(2′)	5065 (2)	2029 (21)	2870 (5)	43 (2)
C(3′)	4793 (3)	3576 (25)	1501 (8)	32 (2)
O(3′)	4982 (2)	5609 (18)	1705 (6)	45 (2)
C(4′)	4477 (2)	4367 (22)	1262 (6)	27 (2)
C(5′)	4291 (3)	3514 (25)	404 (6)	28 (2)
S	4253 (1)	419 (7)	411 (1)	29 (0)
C(γ)	4176 (2)	−224 (23)	−760 (6)	23 (2)
C(β)	4451 (2)	−343 (24)	−1137 (6)	32 (2)
C(α)	4389 (3)	−947 (19)	−2102 (7)	32 (2)
N(α)	4200 (3)	808 (17)	−2609 (5)	37 (2)
C(1)	4271 (2)	−3387 (23)	−2295 (6)	31 (2)
O(1)	4040 (2)	−3678 (19)	−2830 (6)	46 (2)
O(2)	4411 (2)	−5023 (17)	−1914 (7)	55 (3)
		Waters of Crystallization		
O(1)	5000	5749 (25)	5000	43 (3)
O(2)	4906 (3)	7620 (23)	6553 (6)	59 (3)
O(3)	3588 (3)	652 (41)	7587 (13)	88 (7)
O(4)	3054 (3)	7993 (43)	5771 (13)	79 (6)
O(5)	3205 (4)	6151 (46)	8045 (14)	86 (7)
O(6)	3470 (4)	4938 (45)	6615 (12)	89 (7)

[a] Calculated from anisotropic thermal parameters (supplementary material).

The puckering of the ribose ring can be assessed by assuming a C(2′)-endo ⇌ C(3′)-endo equilibrium. The percentage of C(3′)-endo can be estimated by the following formula.[22]

$$\text{C(3′)-endo (\%)} = 100[J_{3'4'}/(J_{1'2'} + J_{3'4'})]$$

The conformation about the exocyclic C(4′)–C(5′) bond can be estimated by the expression:[23]

$$P_{\text{gauche/gauche(g/g)}} = 10[13 - (J_{4'5'} + J_{4'5''})]$$

$$P_{\text{gauche/trans(g/t) or trans/gauche(t/g)}} = 100 - P_{(g/g)}$$

The conformational isomers about the C(α)–C(β) bond in the L-homocysteine moiety can be analyzed by the conventional method. Assuming that the interconversion period between the three isomers about the C(α)–C(β) bond (I, II, and III) is small relative to the lifetime of

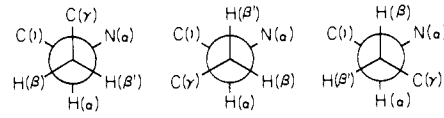

I II III

the individual conformers, the coupling constants may be formulated in terms of their populations, P_{I}, P_{II} and P_{III} as weighted averages:

$$J_{\alpha\beta} = P_{\text{I}}J_{\text{gauche}^+} + P_{\text{II}}J_{\text{gauche}^-} + P_{\text{III}}J_{\text{trans}}$$

$$J_{\alpha\beta'} = P_{\text{I}}J_{\text{gauche}^-} + P_{\text{II}}J_{\text{trans}} + P_{\text{III}}J_{\text{gauche}^-}$$

$$P_{\text{I}} + P_{\text{II}} + P_{\text{III}} = 1$$

From the assumed geometry of the individual conformer, the values of J_{gauche^+} (θ 60°), J_{gauche^-} (θ −60°), and J_{trans} (θ 180°) can be calculated by the following formula:[24]

$$J_{\alpha\beta \text{ or } \alpha\beta'} = 11.0 \cos^2\theta - 1.4 \cos\theta + 1.6 \sin^2\theta$$

Thermal Analysis. The gravimetric and calorimetric changes accompanying thermal dehydration and decomposition were measured by thermogravimetry (TG) and differential thermal analysis (DTA) instruments (Rigaku Denki Co., Japan); Al_2O_3 was the standard compound used for reference. The heating rate was 5 °C/min; samples of 20.0–21.0 mg were used.

X-ray Powder Patterns. These were measured by using a microflex diffractometer (Rigaku Denki Co.) and Cu Kα radiation.

Conformational Energy Calculation. The PPF (partitioned potential energy function) method was used for energy calculations; the total energy (E) of a molecule can be represented by

$$E = E_{\text{nb}} + E_{\text{el}} + E_{\text{t}}$$

where E_{nb}, E_{el}, and E_{t} are the nonbonded, electrostatic, and torsional energies, respectively. These quantities, in units of kcal/mol, can be obtained by computing the following equations:

$$E_{\text{nb}} = \sum_{i>}\sum_{\text{J}}(-A_{ij}R_{ij}^{-6} + B_{ij}R_{ij}^{-12}) \quad (1)$$

$$E_{\text{el}} = \sum_{i}\sum_{j}332.0Q_iQ_jR_{ij}^{-1}\epsilon^{-1} \quad (2)$$

$$E_{\text{t}} = \sum_{k=1}^{N}0.5V_k \times (1.0 + \cos X\theta_k) \quad (3)$$

In eq 1–3, R_{ij} is the observed distance between atoms i and j in Å; A_{ij} and B_{ij} are the coefficients in the Lennard-Jones 6–12 potential function. Q_i is the Coulombic charge on atom i, calculated by the CNDO/2 method;[25] ϵ is the dielectric constant (= 4.0). V_k is the barrier potential for the internal rotation about the *kth* torsion angle (θ_k) (= 2.5 kcal/mol for the C(4′)–C(5′) bond,[26] 2.0 kcal/mol for the C–S bond,[25] 2.7 kcal/mol for the C(α)–C(β) and C(β)–C(γ) bonds[25]). The barrier height of the N(9)–C(1′) and C(α)–C(1) bonds was considered to be negligible.[25,26] X is the periodicity of the barrier (= 3.0), and N is the number of variable torsion angles. The values of A_{ij} and B_{ij} were taken from the literature.[25-28]

For energy minimization, each torsion angle as a variable parameter was optimized by the Powell algorithm.[29] Minimization was carried out by parabola approximation with 4° intervals, and no angle was permitted

(22) D. B. Davies and S. S. Danyluk, *Biochemistry*, **13**, 4417 (1974).
(23) D. J. Wood, F. E. Hruska, R. J. Mynott, and R. H. Sarma, *Can. J. Chem.*, **51**, 2571 (1973).
(24) K. D. Kopple, G. R. Wiley, and R. Tauke, *Biopolymers*, **12**, 627 (1973).
(25) F. A. Momany, R. F. AcGuire, A. W. Burgess, and H. A. Sheraga, *J. Phys. Chem.*, **79**, 2361 (1975).
(26) A. V. Lakshminarayanan and V. Sasisekharan, *Biopolymers*, **8**, 475 (1969).
(27) V. Renugopalakrishnan, A. V. Lakshminarayanan, and V. Sasisekharan, *Biopolymers*, **10**, 1159 (1971).
(28) N. Yathindra and M. Sundaralingam, *Biopolymers*, **12**, 297 (1973).
(29) M. J. D. Powell, *Comput. J.*, **7**, 155 (1964).

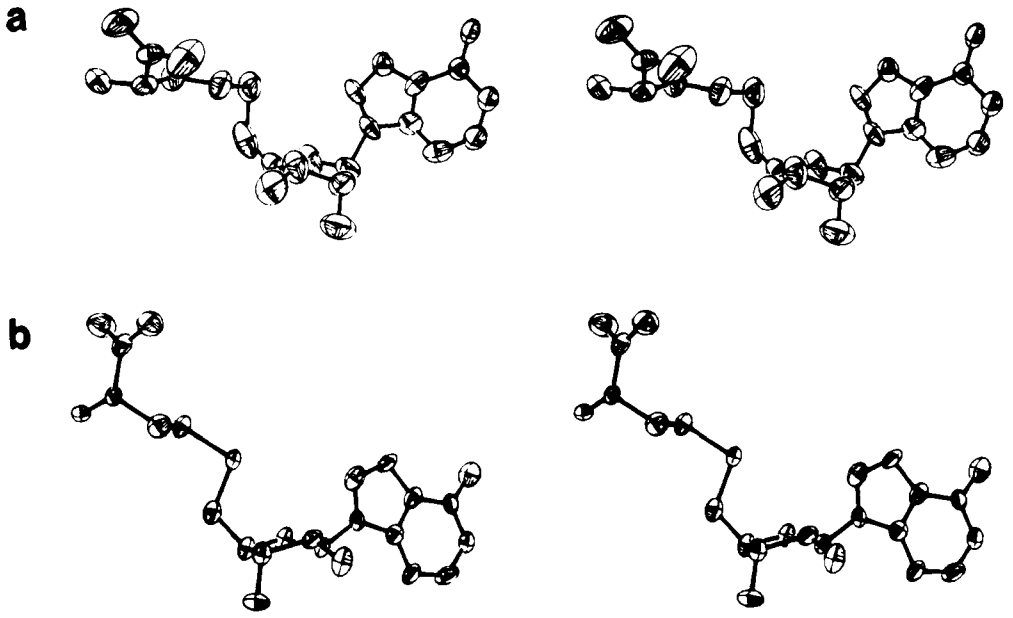

Figure 1. Stereoscopic drawing of the two SAH molecules: (a) molecule A, (b) molecule B. Thermal ellipsoids are drawn at the 50% probability level.

to vary by more than 12° at each step.

Results and Discussion

Molecular Conformation. A table of bond lengths and angles of non-hydrogen atoms is available in the supplementary material. Owing to the relatively low accuracy of the final structural parameters, the quoted values are somewhat uncertain; however, they appear to be normal within standard deviations, compared with those of related compounds.[30-34] A stereoscopic view of two crystallographically independent molecules is shown in Figure 1. The significant difference between the two molecules is in their conformation, especially in the puckering of the ribose ring. The selected torsion angles are listed in Table III.

Ribose Moieties. The puckering of the ribose moieties is best described by the pseudorotation concept.[35] In the ribose ring of molecule A, the pseudorotational phase angle P_r is 24.0°, and the maximum amplitude of puckering τ_m is 32.3°. Thus, the ribose displays the C(3′)-endo (^3E) envelope conformation commonly occurring in type N β-purine nucleosides. On the other hand, the ribose ring of molecule B (P_r = 137.5°, τ_m = 33.2°) is in a C(1′)-exo-C(2′)-endo ($^2T_1$) twist form, which deviates slightly from the range commonly found in type S β-purine nucleosides.[35] These differences are probably ascribable to a particular crystal packing requirement forced on the molecule as well as the hydrogen bondings through the waters of crystallization.

Glycosyl Bonds. The relative orientation of the base with respect to the sugar is described by the glycosyl torsion angle χ_{CN} (O(1′)–C(1′)–N(9)–C(8)). In the SAH crystal, both molecules are in anti with an angle χ_{CN} = 13 (2)° and 51 (2)° for molecules A and B, respectively. These orientations are reasonable because in β-purine nucleosides, the correlation between the glycosyl torsion angle χ_{CN} and ribose puckering shows that C(2′)-endo puckering favors 38° < χ_{CN} < 73° and C(3′)-endo favors −1° < χ_{CN} < 40°.[36,37]

Table III. Selected Torsion Angles (Deg)

		molecule A	molecule B
O(1′)-C(1′)-N(9)-C(4)		−171 (2)	−125 (1)
O(1′)-C(1′)-N(9)-C(8)	χ_{CN}	13 (2)	51 (2)
C(2′)-C(1′)-N(9)-C(4)		70 (2)	116 (1)
C(2′)-C(1′)-N(9)-C(8)		−107 (2)	−69 (2)
C(4′)-O(1′)-C(1′)-C(2′)	τ_0	0 (3)	−30 (1)
O(1′)-C(1′)-C(2′)-C(3′)	τ_1	−20 (2)	33 (1)
C(1′)-C(2′)-C(3′)-C(4′)	τ_2	31 (2)	−24 (1)
C(2′)-C(3′)-C(4′)-O(1′)	τ_3	−32 (2)	8 (1)
C(3′)-C(4′)-O(1′)-C(1′)	τ_4	20 (2)	13 (1)
O(1′)-C(4′)-C(5′)-S		−71 (3)	−59 (1)
C(3′)-C(4′)-C(5′)-S	ψ	41 (3)	63 (1)
C(4′)-C(5′)-S-C(γ)	ϕ	−92 (2)	−157 (1)
N(α)-C(α)-C(β)-C(γ)		−174 (1)	61 (1)
C(1)-C(α)-C(β)-C(γ)	ω_2	66 (2)	−67 (1)
O(1)-C(1)-C(α)-C(β)	ω_1	105 (2)	128 (1)
O(1)-C(1)-C(α)-N(α)		−75 (2)	−53 (2)
C(α)-C(β)-C(γ)-S	ω_3	167 (2)	178 (1)
C(β)-C(γ)-S-C(5′)	ω_4	−89 (2)	82 (1)
N(α)-C(α)-C(1)-O(1)		−13 (2)	0 (2)
N(α)-C(α)-C(1)-O(2)		167 (2)	180 (1)

C(4′)–C(5′) Bonds. The orientations about the C(4′)–C(5′) bond for molecules A and B of SAH are as follows: O(1′)–C(4′)–C(5′)–S = −71 (3)° and −59 (1)°; C(3′)–C(4′)–C(5′)–S = 41 (3)° and 63 (1)°, respectively; i.e., the two crystallographically independent SAH molecules have both gauche/gauche (g/g) conformations, as is common among many of the known β-purine nucleosides, 5′-nucleotides and polynucleotides. This observed conformation is also a preferred one for the SAH molecule, even though it is an unusual nucleoside having a sulfur atom instead of an oxygen atom; in the related molecule, 5′-methylthioadenosine, the conformation is trans/gauche (t/g).[30]

L-Homocysteine Moieties. The conformation is described by five internal rotation angles, ϕ, ω_1, ω_2, ω_3, and ω_4 (see Table III and Figure 7). For molecules A and B, ϕ = −92 (2), −157 (1)°, ω_1 = 105 (2), 128 (1)°, ω_2 = 66 (2), −67 (1)°, ω_3 = 167 (2), 178 (1)°, and ω_4 = −89 (2), 82 (1)°, respectively. Each of these values is reasonable compared to related methionine derivatives,[31,32,38-41]

(30) N. Borkakoti and R. A. Palmer, *Acta Crystallogr., Sect B*, **B34**, 867 (1978).
(31) G. D. Re, E. Gavuzzo, E. Giglio, F. Lelj, F. Massa, and V. Zappia, *Acta Crystallogr., Sect B*, **B33**, 3289 (1977).
(32) S. Neidle and D. Rogers, *J. Chem. Soc. B*, 694 (1970).
(33) R. E. Stenkamp and L. H. Jensen, *Acta Crystallogr., Sect. B*, **B31**, 857 (1975).
(34) J. W. Cornforth, S. A. Reichard, P. Talalay, H. L. Carrell, and J. P. Glusker, *J. Am. Chem. Soc.*, **99**, 7292 (1977).
(35) C. Altona and M. Sundaralingam, *J. Am. Chem. Soc.*, **94**, 8205 (1972).
(36) M. A. Viswamitra, B. S. Reddey, G. H. Lin, and M. Sundaralingam, *J. Am. Chem. Soc.*, **93**, 4565 (1971).
(37) W. Saenger and D. Suck, *Nature (London)* **242**, 610 (1973).
(38) A. Mcl. Mathieson, *Acta Crystallogr.*, **5**, 332 (1952).
(39) A. Aubry, M. Marraud, J. Protas, and J. Néel, *C. R. Hebd. Acad. Seances Sci., Ser. C*, **273**, 959 (1971).
(40) K. Torri and Y. Iitaka, *Acta Crystallogr., Sect. B*, **B29**, 2799 (1973).
(41) R. E. Stenkamp and L. H. Jensen, *Acta Crystallogr., Sect. B*, **B30**, 1541 (1974).

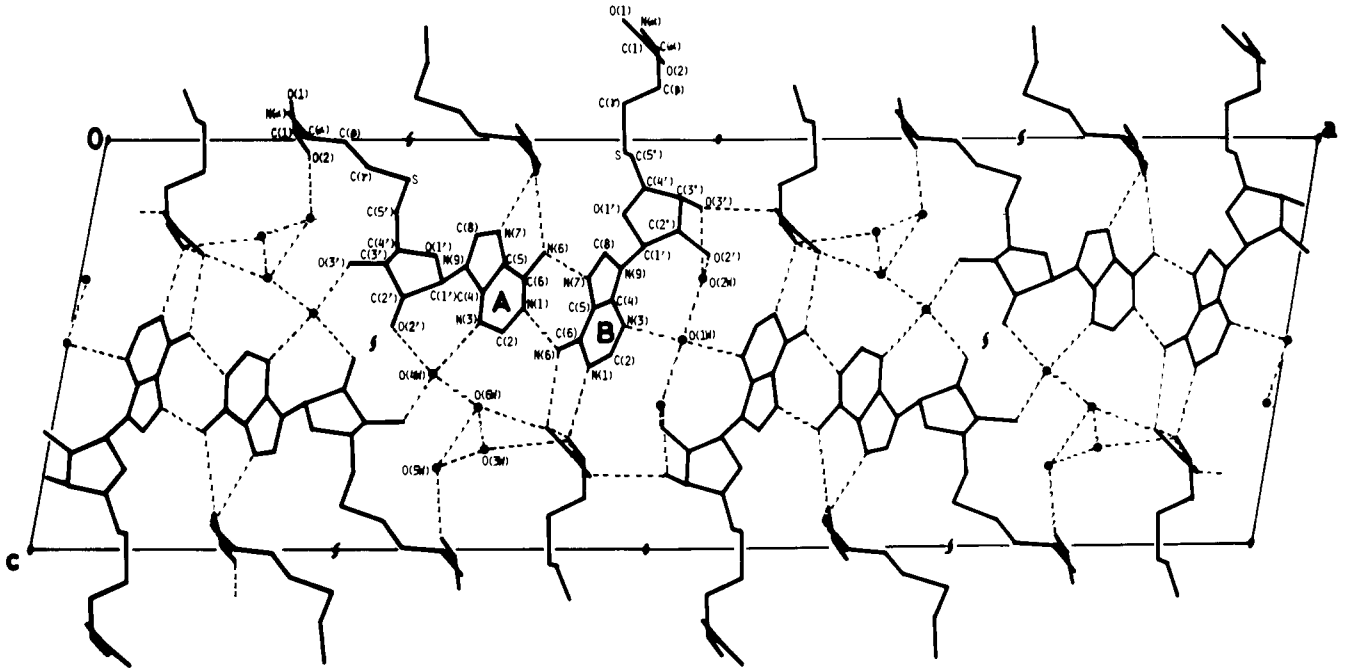

Figure 2. Crystal packing of the molecule viewed along the *b* axis. Dotted lines represent possible hydrogen bonds. Full circules represent waters of crystallization.

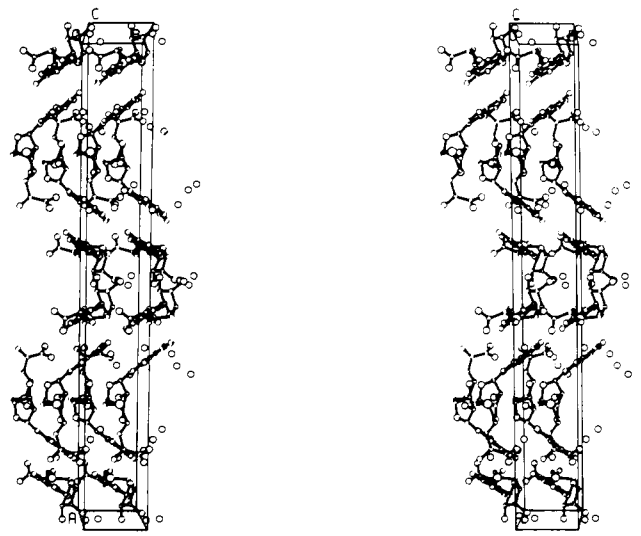

Figure 3. Stereoscopic drawing of the SAH molecules viewed along the *c* axis.

Scheme I

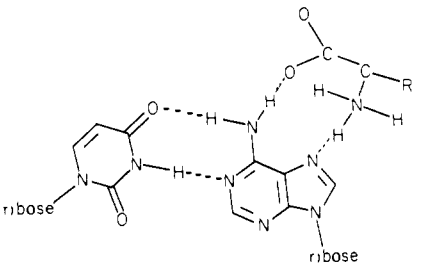

Scheme II

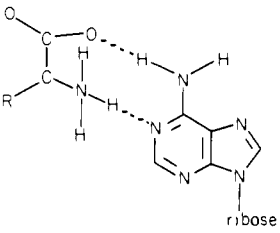

in which ω_1 takes values near 120°, ω_3 near 180° (highly favored), and ω_2 and ω_4 near 60°, 180°, and −60°, although the values of ω_4 tend toward 180° in order to maximize the distance between the non-hydrogen atoms. S, C(γ), C(β), C(α), and N(α) atoms of molecule A form a distorted trans-zigzag chain similar to that found in *S*-methyl-L-methionine chloride[31] (ω_1 = 141.8°, ω_2 = 82.5°, ω_3 = 169.6°, and ω_4 = −72.2°). On the other hand, in molecule B, N(α), C(α), C(1), and O(2) atoms form a trans-zigzag chain that is at almost right angles to the planes consisting of C(α), C(β), C(γ), and S atoms (dihedral angle = 93 (1)°). Therefore, the conformation of molecule A is markedly different from that of molecule B, especially in the torsion angles of ϕ, ω_2, and ω_4. These are sensitive to the crystal packing environment such as interactions with the adjacent adenosine moiety with different ribose puckering and different hydrogen bonding modes with neighboring molecules.

Hydrogen Bonding and Molecular Packing. Figure 2 shows the packing of SAH molecules in the unit cell looking along the shortest *b* axis; a stereoscopic drawing is shown in Figure 3. Owing to the limited data set, not all of the hydrogen atom positions could be located from difference Fourier maps; hydrogen-bond interactions were assigned on the basis of the acceptable short contacts between donor and acceptor atoms. The possible hydrogen bondings are listed in Table IV. Molecules A and B are connected to each other by many hydrogen bonds between the donor and acceptor atoms and via waters of crystallization.

Hydrogen Bonding between SAH Molecules. The adenine bases of molecules A and B are connected to each other by two hydrogen bonds, in which N(1) (molecule A) and N(7) (molecule B) atoms are the acceptors for the amino groups (N(6)). This base-pairing mode is also found in deoxyadenosine monohydrate.[42] Of particular interest is the hydrogen bonding between the α-amino acid moiety and the adenine base (Figure 4). N(6) and N(7) atoms in molecule A and N(6) and N(1) atoms in molecule B are hydrogen bonded to O(1) and N(α) atoms, respectively, of the neighboring molecules. These hydrogen bondings are good models for specific recognition of L-amino acid by nucleic acid bases: the former bonding is a reasonable model for the case in which an

(42) D. G. Watson, D. J. Sutor, and P. Tollin, *Acta Crystallogr.*, **19**, 111 (1969).

Table IV. Hydrogen Bonds

donor	acceptor	symmetry equiv of acceptor	distance, A	angle of O---O-C, N---O-C, or N---N-C, deg
$N(6)^{A}$ [a]	$N(7)^{B}$	$x, 1+y, z$	2.94 (2)	122 (1)
				135 (1)
$N(6)^{A}$	$O(1)^{A}$	$1/2-x, 1/2+y, -z$	2.93 (2)	157 (1)
$O(2')^{A}$	$O(4)^{W}$	$x, -1+y, z$	2.83 (3)	
$O(3')^{A}$	$O(4)^{W}$	$1/2-x, -1/2+y, 1-z$	3.48 (3)	
$N(\alpha)^{A}$	$O(1)^{A}$	$x, -1+y, z$	3.12 (2)	94 (1)
$N(\alpha)^{A}$	$O(2)^{A}$	$x, -1+y, z$	2.89 (2)	105 (1)
$N(\alpha)^{A}$	$N(7)^{A}$	$1/2-x, -1/2+y, -z$	2.88 (2)	113 (1)
				140 (1)
$N(6)^{B}$	$N(1)^{A}$	$x, -1+y, z$	3.08 (2)	112 (1)
				128 (1)
$N(6)^{B}$	$O(1)^{B}$	$x, y, 1+z$	3.04 (2)	122 (1)
$O(2')^{B}$	$O(2)^{W}$	$1-x, -1+y, 1-z$	2.66 (2)	
$O(3')^{B}$	$O(2)^{B}$	$1-x, 1+y, -z$	2.77 (1)	113 (1)
$N(\alpha)^{B}$	$N(1)^{B}$	$x, y, -1+z$	2.87 (2)	112 (1)
				128 (1)
$N(\alpha)^{B}$	$O(1)^{B}$	$x, 1+y, z$	3.23 (2)	89 (1)
$N(\alpha)^{B}$	$O(2)^{B}$	$x, 1+y, z$	2.71 (1)	110 (1)
$O(1)^{W}$	$N(3)^{B}$	$1-x, y, 1-z$	2.82 (2)	102 (1)
				138 (1)
$O(2)^{W}$	$O(3')^{B}$	$1-x, y, 1-z$	2.91 (2)	121 (1)
$O(2)^{W}$	$O(1)^{W}$	$1-x, y, 1-z$	2.75 (2)	
$O(3)^{W}$	$N(\alpha)^{B}$	$x, y, 1+z$	2.88 (3)	115 (1)
$O(3)^{W}$	$O(6)^{W}$	x, y, z	2.87 (3)	
$O(4)^{W}$	$N(3)^{A}$	$x, 1+y, z$	2.82 (3)	119 (2)
				127 (1)
$O(4)^{W}$	$O(6)^{W}$	x, y, z	2.74 (3)	
$O(5)^{W}$	$O(2)^{A}$	$1/2-x, 1/2+y, 1-z$	2.58 (3)	144 (1)
$O(5)^{W}$	$O(3)^{W}$	$x, 1+y, z$	3.26 (3)	
$O(6)^{W}$	$O(1)^{B}$	$x, 1+y, z$	2.72 (3)	156 (1)
$O(6)^{W}$	$O(5)^{W}$	x, y, z	2.81 (3)	

[a] The letters A, B, and W represent molecules A and B of SAH and water of crystallization, respectively.

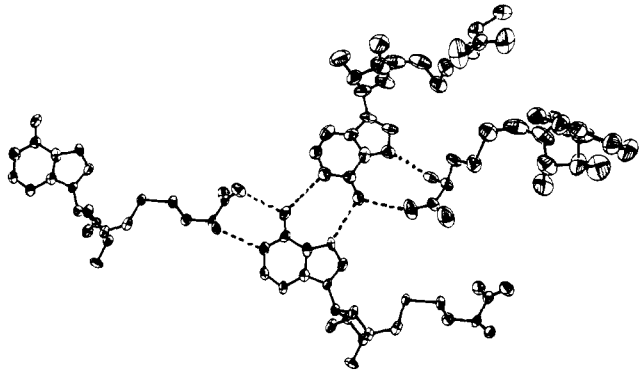

Figure 4. Hydrogen-bonding modes between molecules A and B. Hydrogen bonds are represented by dotted lines.

adenine, base-paired via the N(6) and N(1) atoms to thymine or uracil in the double-stranded DNA or RNA, might form hydrogen bonds with L-amino acid (Scheme I); the latter bonding is a model for the single-stranded DNA- or RNA-L-amino acid interaction (Scheme II).[43] On the basis of their hydrogen bonding modes, the α-amino acid groups of both molecules take zwitterion forms: N(α) atom has three hydrogen bonds with N(7), O(1), and O(2) atoms for molecule A, and bonds with N(1), O(1), and O(2) atoms for molecule B.

Hydrogen Bondings via Waters of Crystallization. All six water sites are located in large gaps; they stabilize the molecular packing of SAH molecules in the crystal lattice via hydrogen bondings with base nitrogen, ribose hydroxyl oxygen, and water oxygen

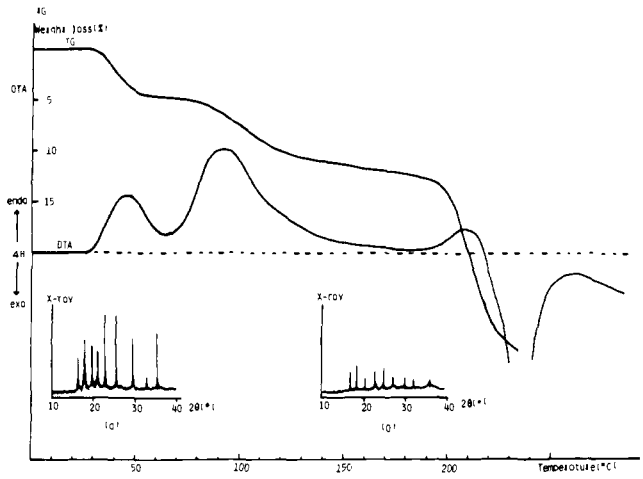

Figure 5. Thermogravimetry (TG) and differential thermal analysis (DTA) profiles and X-ray powder pattern ((a): 20 °C, (b): 140 °C) of SAH crystals.

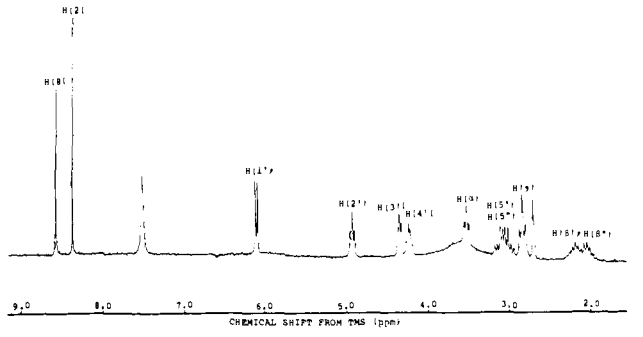

Figure 6. 200-MHz ^1H NMR spectrum of SAH in $(C^2H_3)_2SO$ solution.

atoms. The behavior of water molecules in this crystal was investigated by thermal analysis. The results are shown in Figure 5; the X-ray powder patterns of the hydrated SAH crystal at 20 °C and the dehydrated one at 140 °C are also shown. The dehydration process consisted of two steps: two water molecules estimated from the weight loss were first dehydrated at about 45 °C; the remaining waters were dehydrated at about 90 °C. The former dehydration temperature (45 °C) is fairly low, suggesting that these water molecules, probably O(3W) and O(5W), are loosely bound in the crystal lattice. It is obvious from the X-ray powder patterns of hydrated and dehydrated crystals that dehydration effects a marked structural change, implying that the waters of crystallization are important for the structural stability of this SAH crystal.

Conformation of the SAH Molecule in ^2H_2O and $(C^2H_3)_2SO$ Solutions. ^1H NMR analysis in ^2H_2O solution has already been reported by Stolowitz and Minch;[44] the conformation of SAH takes predominantly C(3')-exo ribose ring, and trans/gauche (t/g) or gauche/trans (g/t) orientation about the C(4')-C(5') bond. However, the ribose ring has been shown to preferentially take a C(2')-endo or C(3')-endo conformation with (g/g) orientation about the C(4')-C(5') bond;[35] this is similar to our X-ray results.

The introduction of the L-homocysteine side chain at the C(5') atom does not seem to affect the conformation of the ribonucleoside moiety in the SAH molecule. Thus, we reexamined its ^1H NMR spectra in ^2H_2O and $(C^2H_3)_2SO$ solutions. Assignment of all proton resonances was made by homonuclear decouplings, spin multiplicities, and comparison with previously published data.[44,45] A ^1H NMR spectrum of SAH in $(C^2H_3)_2SO$ solution is shown in Figure 6; the chemical shifts and coupling constants in $(C^2H_3)_2SO$ and ^2H_2O solutions are given in Table

(43) M. Sundaralingam, "Structure and Conformation of Nucleic Acids and Protein-Nucleic Acid Interactions", M. Sundaralingam and S. T. Rao, Eds., University Park Press, Baltimore, 1975, p 438.

(44) M. L. Stolowitz and M. J. Minch, *J. Am. Chem. Soc.*, **103**, 6015 (1981).

(45) V. N. Rekunova, I. P. Rudakova, and A. M. Yurkevich, *Zh. Obshch. Khim.*, **45**, 2047 (1975).

Table V. Proton Chemical Shifts[a] and Coupling Constants (J)[b] in ^2H_2O and $(C^2H_3)_2SO$ Solutions at 25 °C

	^2H_2O	$(C^2H_3)_2SO$
Chemical Shift, ppm		
H(8)	8.30	8.35
H(2)	8.16	8.15
H(1′)	6.04	5.89
H(2′)	4.84	4.74
H(3′)	4.42	4.16
H(4′)	4.34	4.02
H(5′) (lower field)	3.06	2.92
H(5″) (higher field)	2.98	2.82
H(α)	3.85	3.29
H(β) (lower field)	2.14	1.98
H(β′) (higher field)		1.82
H(γ)	2.72	2.64
Coupling Constant, Hz		
$J_{1'2'}$	5.0	5.8
$J_{2'3'}$	5.2	5.5
$J_{3'4'}$	4.8	4.0
$J_{4'5'}$	5.0	4.0
$J_{4'5''}$	6.5	5.5
$J_{5'5''}$	−14.1	−14.0
$J_{\alpha\beta}$	5.5	5.0
$J_{\alpha\beta'}$	6.5	7.0
$J_{\beta\beta'}$	−13.5	−14.0
$J_{\beta\gamma}$	7.5	6.8

[a] Estimated error, ±0.02 ppm. [b] Estimated error, ±0.2 Hz.

Table VI. Calculated Population (%)[a] of Certain Conformers for SAH Molecule

		this work		Stolowitz and Minch
		^2H_2O	$(C^2H_3)_2SO$	^2H_2O
glycosyl bond	anti	48	35	
ribose ring	C(3′)-endo	49	41	0
C(4′)–C(5′) bond	gauche/gauche	16	35	9
	gauche/trans (trans/gauche)	84	66	91
C(α)–C(β) bond	gauche/gauche	40	40	8
	gauche/trans[b]	36	19	33
	trans/gauche[b]	25	41	59

[a] Error is ±0.5–10%. [b] The values of gauche/trans and trans/gauche are interchangeable.

V. The populations (%) of the conformations about the glycosyl bond, exocyclic C(4′)–C(5′) and C(α)–C(β) bonds, and the ribose puckering are listed in Table VI, as are the values reported by Stolowitz and Minch.[44]

With respect to the conformation about the glycosyl bond, these data show a syn preference of SAH in $(C^2H_3)_2SO$ solution, but equal populations of syn and anti conformers in ^2H_2O solution. On the other hand, in ^2H_2O solution, the SAH molecule exhibits a preference for the (g/t) or (t/g) conformation about the C(4′)–C(5′) bond while it has approximately equal populations of three rotational isomers in $(C^2H_3)_2SO$ solution.

The significant difference between our results and those of Stolowitz and Minch[44] lies in the population of ribose puckering. On the basis of the calculated value obtained by the formula of Davies and Danyluk,[22] there was no prominent preference for the C(3′)-endo or C(2′)-endo conformation, although Stolowitz and Minch report the C(3′)-exo (or C(2′)-endo) conformation to be highly favored. The conformation of the ribose ring is sensitive to the values of $J_{3'4'}$ and $J_{1'2'}$, and their reported value of $J_{3'4'}$ (<0.5) does not coincide with that of our work (= 4.8 Hz in ^2H_2O and 4.0 Hz in $(C^2H_3)_2SO$). The reason for this discrepancy is unclear.

The γ-protons of the L-homocysteine moiety appear as a triplet in both solutions; the βγ coupling is fully described by just one coupling constant, suggesting that the C(β)–C(γ) bond rotates freely, as was described by Stolowitz and Minch.[44] The two

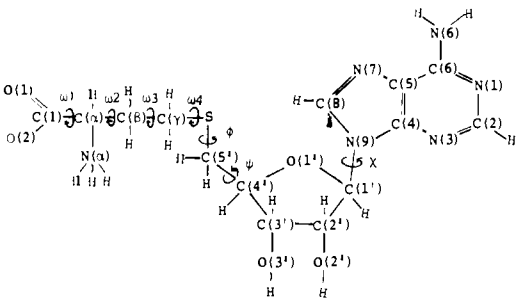

Ribose ring	: C(2′)-*endo*, C(3′)-*endo*
χ(O(1′)-C(1′)-N(9)-C(8))	: 30°, −150°
ψ(C(3′)-C(4′)-C(5′)-S)	: 60°, 180°, −60°
φ(C(4′)-C(5′)-S-C(γ))	: 60°, 180°, −60°
ω1(O(1)-C(1)-C(α)-C(β))	: 120°
ω2(C(1)-C(α)-C(β)-C(γ))	: 60°, 180°, −60°
ω3(C(α)-C(β)-C(γ)-S)	: 180°
ω4(C(β)-C(γ)-S-C(5′))	: 60°, 180°, −60°

Figure 7. Notation of the torsional angles and their starting sets.

β-protons are nonequivalent ($J_{\beta\beta'}$ = −14.0 Hz in $(C^2H_3)_2SO$, −13.5 Hz in ^2H_2O) and have different αβ coupling constants ($J_{\alpha\beta}$ = 5.0 Hz, and $J_{\alpha\beta'}$ = 7.0 Hz in $(C^2H_3)_2SO$, and $J_{\alpha\beta}$ = 5.5 Hz and $J_{\alpha\beta'}$ = 6.5 Hz in ^2H_2O), suggesting the existence of conformational isomers about the C(α)–C(β) bond. While in $(C^2H_3)_2SO$ solution the (g/t) conformer (corresponding to molecule A) or (t/g) conformer exists to the same extent as the (g/g) conformer in molecule B, the latter conformer is slightly preferred in ^2H_2O solution. This contrasts with the findings of Stolowitz and Minch,[44] who reported that SAH exhibits a conformational preference for the (g/t) or (t/g) conformation.

On the basis of ^1H NMR measurements, we propose that the SAH molecule does not exhibit any significant conformational preference (rigidity) as to the adenosine or L-homocysteine moiety in either solution used and that the SAH conformations found in the crystal demonstrate only two isomers among many energetically stable ones.

Conformational Analysis by Classical Potential Energy Calculations. To elucidate the energetically stable conformations of the SAH molecule that could not be unequivocally determined by ^1H NMR study, we carried out conformational analysis by the minimization technique. The requisite structural parameters of the SAH molecule were obtained from our X-ray work and related reports.[25,30-34,46] The nomenclature of the variable torsion angles and their possible starting sets for minimization are shown in Figure 7, where, the basis of various X-ray structural results,[30-34] only one starting angle for ω_1 and ω_3 is given; the other torsion angles have two or three reasonable starting values. Of 324 different sets (2 × 2 × 3 × 3 × 1 × 3 × 1 × 3), some conformers were excluded because they had abnormal steric short contacts. Among energy calculations for different sets with ribose puckering of either the C(2′)-endo or C(3′)-endo form, 10 sets satisfying the energy minimization were found to be stable. These are listed in Tables VII and VIII, together with their torsion angles and final engeries. For each set, the biggest difference between the starting and final torsion angles are in the range of −75° (χ in no. 8) to 47° (χ in no. 1) for the C(2′)-endo conformation (Table VII) and −59° (ω_1 in no. 5) to 28° (χ in no. 5) for the C(3′)-endo conformation (Table VIII).

ψ and φ. Among the seven variable torsion angles, ψ and φ, defining the relative orientation between the adenosine and the L-homocysteine moieties, appear to play an important role in determining the energetically preferable conformations. As is obvious from Tables VII and VIII, three kinds of (ψ,φ) starting sets, (180°, −60°), (60°, 60°), and (180°, 180)°, are the stable SAH conformers. In particular, the (180°, −60°) set seems to be most reasonable for the energetically stable linkage between

(46) A. V. Lakshminarayanan and V. Sasisekharan, *Biochim. Biophys. Acta*, **204**, 49 (1970).

Table VII. Starting and Final Torsion Angles of SAH with C(2')-endo Conformation

no.	starting angles, deg							final angles, deg							energy, kcal/mol
	χ	ψ	ϕ	ω_4	ω_3	ω_2	ω_1	χ	ψ	ϕ	ω_4	ω_3	ω_2	ω_1	
1	30	180	−60	−60	180	180	120	77	195	−56	−60	191	176	112	−37.6
2	−150	180	−60	−60	180	60	120	−123	197	−49	−73	160	55	68	−36.1
3	−150	180	−60	60	180	60	120	−141	198	−64	97	189	64	81	−36.0
4	−150	180	−60	−60	180	180	120	−133	208	−72	−77	179	174	114	−35.4
5	30	180	−60	180	180	−60	120	68	166	−79	182	176	−55	98	−35.1
6	−150	180	−60	180	180	−60	120	−139	191	−49	205	170	−63	93	−35.1
7	30	180	−60	−60	180	−60	120	48	204	−51	−65	176	−61	90	−34.3
8	−150	60	60	180	180	−60	120	−225	48	84	187	205	−54	65	−32.7
9	30	60	60	180	180	−60	120	−13	40	81	155	173	−67	170	−32.7
10	−150	60	60	180	180	60	120	−206	43	85	180	179	48	93	−32.6
crystal (molecule B)								51	63	−157	82	178	−67	128	−29.4

Table VIII. Starting and Final Torsion Angles of SAH with C(3')-endo Conformation

no.	starting angles, deg							final angles, deg							energy, kcal/mol
	χ	ψ	ϕ	ω_4	ω_3	ω_2	ω_1	χ	ψ	ϕ	ω_4	ω_3	ω_2	ω_1	
1	30	60	60	180	180	−60	120	56	63	77	160	167	−69	98	−35.7
2	30	180	−60	−60	180	180	120	39	187	−63	−52	182	174	72	−34.4
3	−150	180	−60	−60	180	−60	120	−151	191	−78	−70	172	−75	72	−34.2
4	−150	180	−60	−60	180	180	120	−156	193	−71	−66	176	170	74	−34.2
5	30	60	60	180	180	180	120	58	57	82	176	177	169	61	−34.2
6	−150	180	−60	−60	180	60	120	−161	189	−77	−73	164	58	77	−33.9
7	−150	180	−60	180	180	−60	120	−150	171	−72	207	176	−56	95	−33.8
8	30	180	−60	−60	180	−60	120	23	192	−66	−54	181	−55	92	−33.8
9	−150	180	180	60	180	60	120	−164	172	185	64	173	63	78	−31.9
10	−150	180	−60	180	180	60	120	−162	172	−83	178	185	62	85	−31.3
crystal (molecule A)								13	41	−92	−89	167	66	105	−30.7

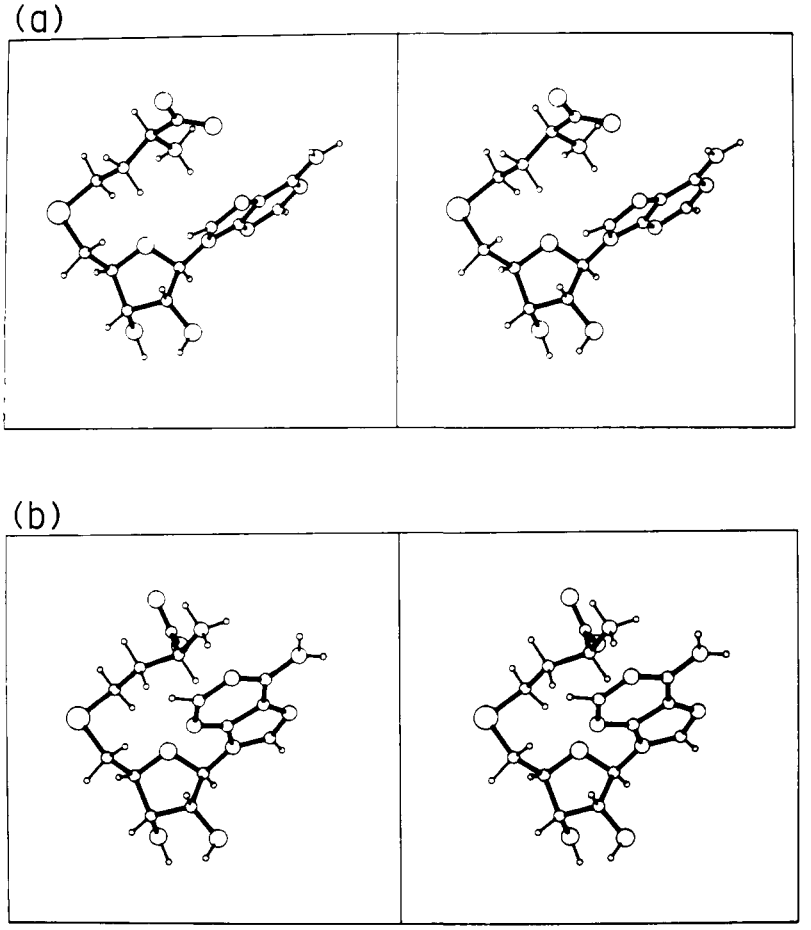

Figure 8. Calculated models of SAH having the energetically stable conformation for C(2')-endo ribose pucker. (a) Set no. 1 of Table VII; (b) set no. 2 of Table VII.

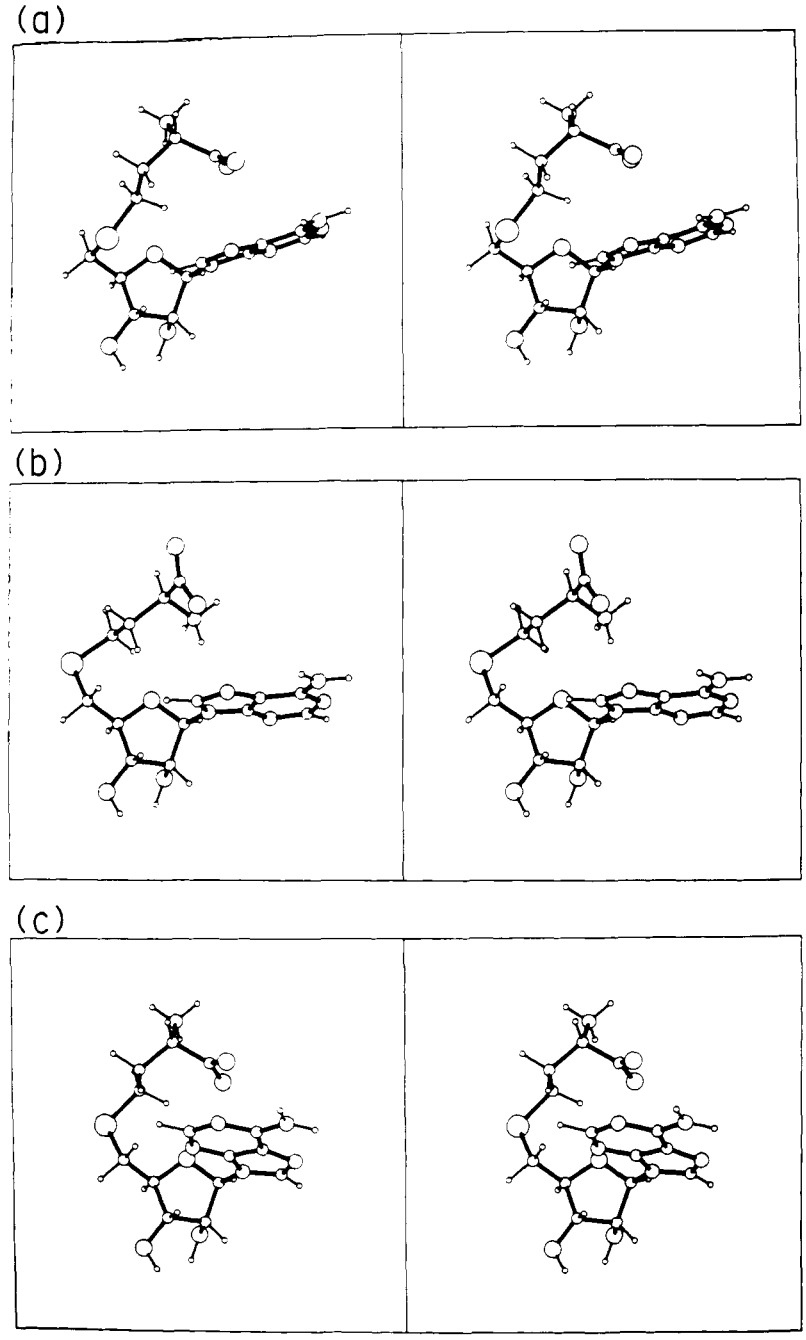

Figure 9. Calculated models of SAH having the energetically stable conformation for C(3′)-endo ribose pucker. (a) Set no. 1 of Table VIII, (b) set no. 2 of Table VIII, (c) set no. 3 of Table VIII.

the L-homocysteine and adenosine moieties having either anti or syn orientation about the glycosyl bond.

Torsion angle ϕ is highly dependent on the torsion angle ψ. Possibly, the reason the conformation about the exocyclic C(4′)–C(5′) bond favors the (g/t) orientation (ψ = 180°), particularly in the C(2′)-endo conformation, may be that the bulky S atom may take the orientation to avoid steric hindrance with the adenine base. On the other hand, C(3′)-endo ribose puckering is spatially more allowable for the (g/g) orientation about the C(4′)–C(5′) bond, as seen in set no. 1 of Table VIII. The (t/g) orientation of ψ (= −60°) seems to be less favorable for stable SAH conformation.

χ Value. The χ value starting at 30° or −150° was converted to the anti or syn region for all of the stable conformations, irrespective of its considerable change during energy minimization. It is important to note that in stable conformers, the syn orientations about the glycosyl bond are found to the same extent as anti orientations, although X-ray study suggested a preference for anti conformation. In particular, the syn conformation seems to be preferred in the C(2′)-endo conformations, although the most stable one is in the anti region.

Ribose Ring. The C(2′)-endo ribose pucker is energetically more stable by about 2 kcal/mol than the pucker with C(3′)-endo form. Interestingly, the former highly favors the (g/t) orientation about the ψ angle, irrespective of the χ value (−34 to −38 kcal/mol), while C(3′)-endo puckering allows the (g/g) as well as the (g/t) orientation.

L-Homocysteine Moiety. It is noteworthy that of the two torsion angles, ω_1 and ω_3, which were selected at 120° and 180° as the most reasonable starting value, the ω_1 angle was changed without exception to the lower value (ranging from 60° to 110°), probably to avoid the steric short contact between the α-carboxyl oxygen (O(1)) and α-amino nitrogen (N(α)) atoms. The ω_3 angle did not change; it plays an important role for determining the energetically stable conformation of the L-homocysteine moiety, because if the sets with either 60° or −60° as the starting angle of ω_3 were used, we obtained only energetically unstable conformers (energy values: −16.2 to −28.4 kcal/mol). On the other hand,

no conformational preference in the torsion angles of ω_2 and ω_4 was observed: conformers with gauche$^+$ (g^+), gauche$^-$ (g^-), and trans (t) existed to almost the same extent in the stable SAH conformers. Therefore, these torsion angles are conformationally flexible.

Energetically Stable SAH Conformation and Its Biological Implication. The conformation of the SAH molecule can be characterized by the ribose puckering and seven torsion angles. Among these, the combination of χ, ψ, and ϕ torsion angles may be highly important for the energetically favored conformers having either C(2')-endo or C(3')-endo ribose puckering. From the calculated energy listed in Tables VII and VIII, the stable conformation could be divided into the following sets of (χ,ψ,ϕ): (anti,(g/t),g$^-$) and (syn,(g/t),g$^+$) for C(2')-endo ribose pucker; anti,(g/g),g$^+$), (anti,(g/t),g$^-$), and (syn,(g/t),g$^-$) for C(3')-endo pucker. The most stable conformers belonging to the respective ribose puckering are shown in Figures 8 and 9. These five stable SAH conformers, obtained by energy calculations, coincide with the data obtained from ^{1}H NMR spectra, which provide information as to the averaged conformation. On the other hand, the conformation observed in the crystal structure is also in the region having energy minima (−30.7 kcal/mol for molecule A and −29.4 kcal/mol for molecule B). These conformers may represent slightly unfavored ones upon interaction between the neighboring molecules accompanying the crystal packing.

The functional groups of primary importance for the binding to methyltransferases are terminal carboxyl (O(1) and O(2)) and amino (N(α)) groups, sulfur atom (S), the amino nitrogen atom of adenine base (N(6)), and the 3'- and 2'-hydroxyl groups of ribose ring (O(2') and O(3')). Binding may require the energetically most stable conformer; therefore, we propose that the conformer shown in Figure 8a may be the most likely candidate of the SAH molecule required for binding to the methyltransferases. This hypothesis is based on the opinion that the energy value (−37.6 kcal/mol) can reasonably be regarded as significantly stable compared with the other conformers shown in Figures 8b and 9 (−34.2 to 36.1 kcal/mol). It is interesting to note that the conformer shown in Figure 8a is compactly folded and that all of its functional groups protrude to the surface, resulting in the capacity for hydrogen bondings with the functional groups at the binding site of methyltransferases.

The functional groups of SAM essential for binding to methyltransferases have been determined by synthetic procedures,[47,48] and the groups effective in methyl donor activity are identical with those that in SAH are necessary for binding to the enzymes. This observation and the potent inhibition of methyltransferases by SAH, a metabolite of SAM, imply that the spatial conformation of SAH at the active site must be identical with that of SAM, except in the configuration of the sulfonium center. As the sulfonium atom of the SAM molecule takes the S configuration,[34] methylation by methyltransferases at the sulfur atom for the conformer shown in Figure 8a would be stereochemically most preferable. There are no short contacts between the methyl group and L-homocysteine or the adenosine moiety. Further physicochemical investigations are required to support these suggestions.

Acknowledgment. We are indebted to Dr. M. Sugiura, Kobe Women's College of Pharmacy, for the measurements of 200-MHz NMR spectra.

Supplementary Material Available: Tables of observed and calculated structure factors, anisotropic thermal parameters, and the bond lengths and angles of non-hydrogen atoms (14 pages). Ordering information is given on any current masthead page.

(47) V. Zappia, C. R. Zydek-Cwick, and F. Schlenk, *J. Biol. Chem.*, **244**, 4499 (1969).
(48) R. T. Borchardt, Y. S. Wu, J. A. Huber, and A. F. Wycpalek, *J. Med. Chem.*, **19**, 1104 (1976).

Stereoelectronic and Conformational Effects in Meisenheimer Complexes. Intrinsic Reactivities of Spiro vs. 1,1-Dimethoxy and 1-Methoxy-1-phenoxy Complexes[1]

Claude F. Bernasconi* and Keith A. Howard

Contribution from the Thimann Laboratories of the University of California, Santa Cruz, California 95064. *Received April 1, 1982*

Abstract: Rate and equilibrium constants of formation of spiro Meisenheimer complexes derived from 1-(2-hydroxyethoxy)-2,6-dinitro-4-X-benzenes in aqueous solution are compared with those for 1,1-dimethoxy Meisenheimer complexes derived from 2,6-dinitro-4-X-anisoles. Hammett ρ values for the equilibrium constants are 8.2 for the dimethoxy and 5.9 for the spiro complexes, while the normalized ρ values for the rate constants of complex formation (cleavage) are 0.44 (−0.56) for the dimethoxy and 0.58 (−0.42) for the spiro complexes. The large difference in the equilibrium ρ values is attributed to a conformation of the dimethoxy complexes in which there is repulsion between the lone pairs on the ketal and the *o*-nitro group oxygens. A procedure for making the reactions in the two families thermodynamically comparable by correcting the rate and equilibrium constants for the pK_a difference in the nucleophile and for the intramolecularity of spiro complex formation was applied. The corrected parameters show that the spiro complexes form and decompose much faster than the dimethoxy complexes. This enhanced reactivity, $\Delta\Delta G^{\ddagger}$, is attributed to a stereoelectronic effect or p–π overlap between a lone pair orbital of the nonreacting oxygen and the benzene ring, which is only feasible in the transition state of the spiro complex reaction (**14**) but not in the transition state of the dimethoxy complex reaction (**15**). This interpretation is strongly supported by the fact that $\Delta\Delta G^{\ddagger}$ increases with increasing electron-withdrawing strength of the X substituent. The enhanced rate of formation and decomposition of the spiro complex from catechol 2,4,6-trinitrophenyl ether compared to that of the corresponding 1-methoxy-1-phenoxy complex can be explained in a similar way.

There is a striking difference between the intrinsic reactivities of 1,1-dimethoxy and of spiro Meisenheimer complexes.[2] The work to be described in this paper is aimed at obtaining a more quantitative measure of this difference, at sorting out transi-

0002-7863/82/1504-7248$01.25/0